Flexocoupling impact on size effects of piezoresponse and conductance in mixed-type ferroelectric semiconductors under applied pressure

Anna N. Morozovska, Eugene A. Eliseev, Yuri A. Genenko, Ivan S. Vorotiahin, Maxim V. Silibin, Ye Cao, Yunseok Kim, Maya D. Glinchuk, and Sergei V. Kalinin

Phys. Rev. B **94**, 174101 — Published 2 November 2016

DOI: 10.1103/PhysRevB.94.174101

Quantifying the role of flexoelectricity on piezoresponse and conductance in mixed-type ferroelectrics-semiconductors: pressure and size effects

Anna N. Morozovska[1,*], Eugene A. Eliseev [2], Yuri A. Genenko[3†], Ivan S. Vorotiahin[1, 3], Maxim V. Silibin[4], Ye Cao[5], Yunseok Kim[6], Maya D. Glinchuk [2], and Sergei V. Kalinin[5‡]

[1] *Institute of Physics, National Academy of Sciences of Ukraine, 46, pr. Nauky, 03028 Kyiv, Ukraine*

[2] *Institute for Problems of Materials Science, National Academy of Sciences of Ukraine, Krjijanovskogo 3, 03142 Kyiv, Ukraine*

[3] *Institut für Materialwissenschaft, Technische Universität Darmstadt, Jovanka-Bontschits-Str. 2, 64287 Darmstadt, Germany*

[4] *National Research University of Electronic Technology "MIET", Bld. 1, Shokin Square, 124498 Moscow, Russia*

[5] *The Center for Nanophase Materials Sciences, Oak Ridge National Laboratory, Oak Ridge, TN 37831*

[6] *School of Advanced Materials Science and Engineering, Sungkyunkwan University (SKKU), Suwon 16419, Republic of Korea*

Abstract

We explore the role of flexoelectric effect in functional properties of nanoscale ferroelectric films with mixed electronic-ionic conductivity. Using coupled Ginzburg-Landau model, we calculate spontaneous polarization, effective piezo-response, elastic strain and compliance, carrier concentration and piezo-conductance as a function of thickness and applied pressure. In the absence of flexoelectric coupling, the studied physical quantities manifest well-explored size-induced phase transitions, including transition to paraelectric phase below critical thickness. Similarly, in the absence of external pressure flexoelectric coupling affects properties of these films only weakly. However, the combined effect of flexoelectric coupling and external pressure induces polarizations at the film surfaces, which cause the electric built-in field that destroys the thickness-induced phase transition to

* corresponding author 1, e-mail: anna.n.morozovska@gmail.com
† corresponding author 2, e-mail: genenko@mm.tu-darmstadt.de
‡ corresponding author 3, e-mail: sergei2@ornl.gov

paraelectric phase and induces the electret-like state with irreversible spontaneous polarization below critical thickness. Interestingly, the built-in field leads to noticeable increase of the average strain and elastic compliance in this thickness range. We further illustrate that the changes of the electron concentration by several orders of magnitude under positive or negative pressures can lead to the occurrence of high- or low-conductivity states, i.e. the nonvolatile piezo-resistive switching, in which the swing can be controlled by the film thickness and flexoelectric coupling. Obtained theoretical results can be of fundamental interest for ferroic systems, and can provide theoretical model for explanation of a set of recent experimental results on resistive switching and transient polar states in these systems,

I. Introduction

Ferroelectric materials have long remained the focus of theoretical and experimental research due to their unique functional properties. These include strong electromechanical coupling that enables applications in sensors and actuators [1], and presence of equivalent polar states that enables multiple types of ferroelectric memories [2, 3]. In the 15 years, much attention have been focussed ofn the multiferroic materials combining ferroelectric and magnetic functionalities [4, 5]. Finally, in the last several years, the attention of condensed matter physics and materials community has been riveted to applications combining ferroelectric, ionic, and electronic functionalities of these materials [6, 7, 8, 9, 10]. Consequently, investigation of electromechanical, electrochemical and electrophysical properties of nanosized ferroelectrics-semiconductors with mixed type ionic-electronic conductivity (**FeMIECs**) is of significant interest for both fundamental science and numerous applications. Although FeMIECs in the form of thin films and nanocomposites are among the most promising MIECs materials for the next generation of nonvolatile, resistive and memristive memories, logic devices, ultrasensitive sensors, miniature actuators and positioners [11, 12, 13], the physical principles of the complex interplay between the ferroelectric polarization, elastic strains, ionic and electronic state at the nanoscale are not clear so far. This lack of physical understanding precludes the successful implementation of FeMIECs in the aforementioned applications.

Futhermore, emergence of scanning probe microscopy tools have made the studies of coupled electormehcnical and conductive phenomena nearly routine. Multiple studies of electromechanical responses (**piezo-response**) by Electrochemical Strain Microscopy (ESM) [14, 15, 16] and Piezoresponse Force Microscopy (PFM) [17] and local conductivity by Current Atomic Force Microscopy (C-AFM) [18] and related techniques [19, 20, 21, 22] revealed that their electro-conductance is strongly coupled with polar and elastic states. Moreover, both SPM and interferometric measurements with high sub-nm resolution indicate the important role of the local gradients of polarization, strain and space charge density in the formation of aforementioned local response [14-18]. The local gradient of polarization induces elastic strain, and vice versa, the gradient of elastic stress induces electric field due to the flexoelectric coupling (**flexocoupling**) [23, 24]. The gradients inevitably cause the space charge redistribution in MIECs and FeMIECs via several mechanisms [25, 26], including electromigration and diffusion [27, 28], chemical strains and stresses [29, 30, 13], and deformation potential [31, 32]. Generally, these effects are strongly coupled in a ferroelectric and cannot be separated *a priori*. However, the following important aspects should be mentioned.

One important aspect of material behaviour on the nanoscale is the emergence of flexoelectric coupling [33, 34]. The strong strain gradients are inevitably present near the surfaces, in thin films [35, 36, 37], nanoparticles [38] and fine-grained ceramics [39, 40]. Therefore the role of flexocoupling in the formation of piezo-response and piezo-conductance can essentially increase due to the intrinsic size

effects, which become pronounced when the thickness of investigated FeMIEC film becomes less than 50 nm. While the role of flexoeffect in SPM measurements have been discussed as early as 2006 [41, 42], recently it has become a mainstream explanation for a broad set of functional observations. While very significant doubts have been raised [43], it remains an important aspect of these systems.

Second important aspect of ferroelectricity in the nanoscale systems is the ferroelectric size effect. The intrinsic size effect in thin ferroelectric films manifests as the disappearance of ferroelectric phase when the film thickness becomes smaller than the critical thickness [44]. The critical thickness depends on the polarization direction, correlation length, surface energy contribution, electrical and mechanical conditions at the film surfaces [45, 46, 47, 48]. Here, the surface energy determines the value of the so-called extrapolation lengths [45]. Depolarization field is originated from nonzero divergence of polarization vector, as well as from the incomplete screening of the polarization bound charges by the electrodes [45, 48]. Elastic strains are caused by e.g. film and substrate lattice mismatch [46, 47]. All these factors, which are closely related to the surface influence, often lead to the appearance of a developed polarization gradient from the film surface towards its center. Note that in the comprehensive description the polarization gradient induces elastic strain due to the flexoelectric coupling, suggesting the potential interplay between the two.

Finally, the third aspect of thin film behaviour is surface piezoelectric effect caused by inversion symmetry breaking in the direction normal to the surface. Surface piezoeffect coupled with misfit strain leads to the appearance of built-in electric field that in turn destroys the size-induced phase transition into a paraelectric phase at the critical thickness and induces the electret-like state with irreversible polarization at film thickness less than the critical one [46, 47].

These considerations necessitate the theoretical modeling of the flexocoupling impact on the size effects of the spontaneous polarization, effective piezo-response, elastic strain and compliance, carrier concentration and piezo-conductance in thin films of FeMIECs under applied pressure. Here we analyze these phenomena in the framework of Landau-Ginzburg-Devonshire (LGD) theory [25-27, 38 49, 50].

II. Problem statement and basic equations

Generalized expression for the Landau-Ginzburg-Devonshire (LGD)-type Gibbs potential of the spatially confined ferroelectric mixed-type semiconductors, that is the sum of the bulk (G_V) and surface (G_S) parts, has the following form [26, 51]:

$$G_V = \int_V d^3r \begin{pmatrix} \frac{a_{ik}}{2} P_i P_k + \frac{b_{ijkl}}{4} P_i P_j P_k P_l + \frac{g_{ijkl}}{2} \left(\frac{\partial P_i}{\partial x_j} \frac{\partial P_k}{\partial x_l} \right) - P_i E_i - Q_{ijkl} \sigma_{ij} P_k P_l - \frac{s_{ijkl}}{2} \sigma_{ij} \sigma_{kl} \\ - F_{ijkl} \sigma_{ij} \frac{\partial P_l}{\partial x_k} - \left(\Sigma_{ij}^e \delta n + W_{ij}^d \delta N_d^+ \right) \sigma_{ij} + e\varphi \left(Z_d N_d^+ - n \right) \\ - N_d^+ E_d - TS_d \left[N_d^+ \right] + nE_C - TS_{el}[n] + \frac{3k_B T}{2} N_C F_{3/2} \left(\frac{E_g + e\varphi}{k_B T} \right) \end{pmatrix} \quad (1a)$$

$$G_S = \sum_m \int_{Sm} \left(\frac{A_{jk}^m}{2} P_j P_k + d_{jkl}^{Sm} u_{jk}^{Sm} P_l \right) d^2 r \quad (1b)$$

Here, the summation is performed over all repeating indexes; P_i is a ferroelectric polarization, $E_i = -\partial\varphi/\partial x_i$ is a quasi-static electric field, φ is the electric potential. The coefficients of LGD potential expansion on the polarization powers are $a_{ik} = \alpha_{ik}^T (T - T_c)$ and b_{ijkl}, T is the absolute temperature, T_c is the Curie temperature. This choice of LGD expansion corresponds to materials with inversion center in the parent phase (e.g. with cubic parent phase). Elastic stress tensor is σ_{ij}, Q_{ijkl} is electrostriction tensor, F_{ijkl} is the flexoelectric effect tensor [52], g_{ijkl} is gradient coefficient tensor**,** s_{ijkl} is elastic stiffness.

Variations of the electron density, and ionized donor concentration are $\delta n(\mathbf{r}) = n(\mathbf{r}) - n_0$ and $\delta N_d^+(\mathbf{r}) = N_d^+(\mathbf{r}) - N_{d0}^+$. Constant values of n_0 and N_{d0}^+ correspond to stress-free reference state at zero electric field. e is the electron charge, Z_d is the donor ionization degree. Deformation potential tensor is denoted by Σ_{ij}^e and Vegard expansion (or elastic dipole) tensor is W_{ij}^d [29, 30]. The Vegard tensor W_{ij}^d for donors will be regarded diagonal. Only ionized donors (e.g. impurity ions or oxygen vacancies) are regarded mobile [53]. Mobile acceptors can be considered in a similar way. E_d is the donor level, E_C is the bottom of the conduction band.

The entropy of ionized donors is estimated under the approximation of an infinitely thin single donor level, as

$$S_d \left[N_d^+ \right] = -k_B \left(N_d^0 \left(\frac{N_d^+}{N_d^0} \ln\left(\frac{N_d^+}{N_d^0} \right) + \left(1 - \frac{N_d^+}{N_d^0} \right) \ln\left(1 - \frac{N_d^+}{N_d^0} \right) \right) \right), \quad (2a)$$

where N_d^0 is the concentration of donor atoms. The entropy density of electron Fermi gas, considered in the parabolic or effective mass approximation, is

$$S_{el}[n] = -k_B N_C \int_0^{n/N_C} d\tilde{n} F_{1/2}^{-1}(\tilde{n}), \quad (2b)$$

where $F_{1/2}^{-1}(\xi)$ is the inverse function to the Fermi ½-integral $F_{1/2}(\xi)=\frac{2}{\sqrt{\pi}}\int_0^\infty \frac{\sqrt{\zeta}d\zeta}{1+\exp(\zeta-\xi)}$ (see **Appendix A** of **Suppl. Mat**. [54]). $N_C=\left(m_n k_B T/\left(2\pi\hbar^2\right)\right)^{3/2}$ is the effective density of states in the conduction band, electron effective mass is m_n [55]. The partial derivative $\partial S_{el}/\partial n=-k_B F_{1/2}^{-1}\left(n/N_C\right)$. For analytical estimates, we use approximations for direct and inverse Fermi integrals, $F_{1/2}(\varepsilon)\approx\left(\exp(-\varepsilon)+\left(3\sqrt{\pi}/4\right)\left(4+\varepsilon^2\right)^{-3/4}\right)^{-1}$ and $F_{1/2}^{-1}(\tilde{n})\approx\left(3\sqrt{\pi}\tilde{n}/4\right)^{2/3}+\ln\left(\tilde{n}/(1+\tilde{n})\right)$ correspondingly. These are valid in a wide range of ε and $\tilde{n}$ values [56]. The last term, in Eq.(1a), is the electron kinetic energy [51], $F_{3/2}(\xi)=\frac{2}{\sqrt{\pi}}\int_0^\infty \frac{\zeta\sqrt{\zeta}d\zeta}{1+\exp(\zeta-\xi)}$ is the Fermi 3/2-integral.

The surface properties are described by the constants A_{ij}^{Sm} , the surface dielectric stiffness at the surface S_m, d_{ijk}^S is the surface piezoelectric tensor, u_{ij}^S is the surface strain field, originated from e.g. film and substrate lattice mismatch [46]. The surface piezoeffect could be essential at distances of order 1-5 lattice constants from the film surface [57], although for strong enough film-substrate lattice mismatch it can be the source of thin film self-polarization (see [46, 47] and refs therein). We will not consider the latter case here and refer it to future studies.

For ferroelectrics with cubic parent phase the term $Q_{ijkl}P_k P_l$ automatically includes piezoelectric contribution, because the polarization change under electric field E_m can be approximated as [58]

$$P_k^t=P_k\left(E_m\right)+\varepsilon_0\left(\varepsilon_{km}^b-\delta_{km}\right)E_m\approx P_k^S+\varepsilon_0\left(\varepsilon_{km}^f-\delta_{km}\right)E_m. \quad (3a)$$

Here P_k^S is a spontaneous polarization component, ε_0 is the dielectric permittivity of vacuum, δ_{km} is a Kroneker symbol and ε_{ij}^f is the relative dielectric permittivity of ferroelectric that includes a soft-mode related electric field-dependent contribution ε_{ij}^{sm} and an electric field-independent lattice background contribution ε_{ij}^b [35]. Consequently, an apparent piezoelectric coefficient becomes [59]

$$d_{ijk}=2\varepsilon_0\left(\varepsilon_{km}^f-\delta_{km}\right)Q_{ijml}P_l^S. \quad (3b)$$

As a relevant experimental geometry, we consider the case of flattened tip or a thin disk electrode placed in an electric contact with a ferroelectric mixed-type semiconductor film clamped to a rigid bottom electrode. One-component polarization P_3 is normal to the film surface, corresponding to a tetragonal ferroelectric phase in a c-domain film. Problem geometry is shown in **Figure 1.** One-dimensional approximation of capacitor geometry is applicable for the problem solution, if the radius of the top disk electrode is much larger than the film thickness.

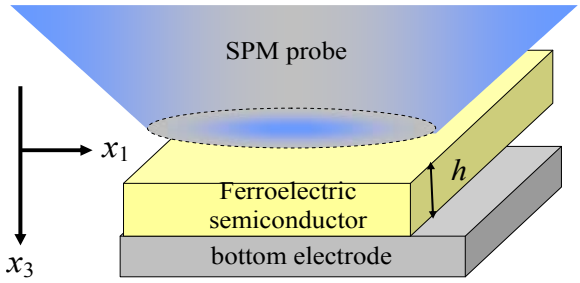

Figure 1. Geometry of the considered problem. We consider the situation when either the radius of the SPM tip is much larger than the film thickness, or the ambient screening charges play the role of a top electrode.

For the semiconductor film with mixed ionic-electronic conductivity the electric potential φ can be found self-consistently from the Poisson equation

$$\varepsilon_0 \varepsilon_{33}^b \frac{\partial^2 \varphi}{\partial x_3^2} = \frac{\partial P_3}{\partial x_3} - e\left(Z_d N_d^+(\varphi) - n(\varphi)\right) \tag{4}$$

with boundary conditions corresponding to the fixed potentials at the electrodes, $\varphi(0) = V$, $\varphi(h) = 0$, including the short-circuited case, $\varphi(0) = \varphi(h) = 0$. Here V is the applied voltage. In Equation (4) we used the relation (3a) between the total and ferroelectric polarization contributions.

When the system is in thermodynamic equilibrium, currents are absent and electrochemical potentials are equal to the Fermi level. In the considered case donor concentration is $N_d^+ = N_d^0\left(1 - f\left(\left(E_d + W_{ij}^d \sigma_{ij} - eZ_d\varphi + E_F\right)/k_B T\right)\right)$, where the Fermi-Dirac distribution function is introduced as $f(x) = (1+\exp(x))^{-1}$ and E_F is the Fermi energy level in equilibrium. Electron density is $n = N_C F_{1/2}\left(\left(e\varphi + \Sigma_{ij}^e \sigma_{ij} + E_F - E_C\right)/k_B T\right)$, where $F_{1/2}(\xi) = \frac{2}{\sqrt{\pi}}\int_0^\infty \frac{\sqrt{\zeta}d\zeta}{1+\exp(\zeta-\xi)}$ is the Fermi ½-integral.

Inhomogeneous spatial distribution of the ferroelectric polarization component(s) is determined self-consistently from the LGD-type Euler-Lagrange equations,

$$\frac{\delta G}{\delta P_i} - \frac{\partial}{\partial x_k}\left(\frac{\delta G}{\delta(\partial P_i/\partial x_k)}\right) = 0, \tag{5a}$$

with boundary conditions at surfaces S_1 at x_3=0 and S_2 at x_3=h,

$$\left(A_{33}^{S1} P_3 - g_{33}\frac{\partial P_3}{\partial x_3} + F_{kl33}\sigma_{kl}\right)\Big|_{x_3=0} = 0, \tag{5b}$$

and

$$\left(A_{33}^{S2} P_3 + g_{33}\frac{\partial P_3}{\partial x_3} - F_{kl33}\sigma_{kl}\right)\Big|_{x_3=h} = 0, \tag{5c}$$

which follow from the minimization of the Gibbs potential (1). The conditions are of the third kind due to the flexoelectric effect contribution. The explicit form of Euler-Lagrange equations and boundary conditions are listed in the **Appendix B** of **Suppl. Mat** [54]**.** Note that the product $F_{kl33}\sigma_{kl}/A_{33}^{Si}$ act as a surface polarization. The coefficients A_{33}^{S1} and A_{33}^{S2} conditioned by the interface chemistry can be very different for the probed surface $x_3 = 0$, where an active chemical environment can exist, and for the electroded surface $x_3 = h$, where the perfect electric contact is present, as will be considered elsewhere [60].

Equation of state for elastic fields, $\delta G/\delta\sigma_{ij} = -u_{ij}$, obtained from the variation of the functional (1), shows that there are four basic contributions to the elastic strain of the spatially-confined ferroelectric materials with mobile charge species, namely purely elastic, flexoelectric, Vegard and electrostriction contributions. Hence the local strain is

$$u_{ij} = s_{ijkl}\sigma_{kl} + F_{ijkl}\frac{\partial P_k}{\partial x_l} + W_{ij}^{d}\left(N_d^{+} - N_{d0}^{+}\right) + \Sigma_{ij}^{e}\left(n - n_0\right) + Q_{ijkl}P_k P_l \ , \qquad (6)$$

The piezoelectric contribution is automatically included in the relation (6) as linearized electrostriction in the ferroelectric phase accordingly to Eq.(3a), and the apparent piezoelectric coefficient d_{ijk}^{eff} can be introduced according to Eq.(3b).

Generalized Hooke's relations (6) should be supplemented by the mechanical equilibrium equations $\partial\sigma_{ij}/\partial x_j = 0$ in the bulk and equilibrium conditions $\sigma_{ij}n_j\big|_{S_f} = -p_i^{ext}$ at the free surfaces S_f of the system, n_j is the component of the outer normal **n**=(0,0,–1) to the surface S_f [61]. Here we suppose that external pressure p_i^{ext} can be applied to the system. Elastic displacement is zero at the clamped surfaces S_c, $u_i(S_c) = 0$. The evident expressions for elastic strains and stresses are listed in the **Appendix B** of **Suppl. Mat.** [54]

The film surface displacement is $u_3 = \int_0^h u_{33}dx_3$ for the considered geometry. The strain u_{33} is listed in **Appendix B** of **Suppl. Mat** [54]. The average strain $\langle u_{33}\rangle = \frac{u_3}{h}$ has the following form:

$$\langle u_{33}\rangle = -s_{33}^{eff}p_{ext} + W_{33}^{eff}\langle\delta N_d^{+}\rangle + \Sigma_{33}^{eff}\langle\delta n\rangle + \frac{F_{33}^{eff}}{h}\left(P_3(h) - P_3(0)\right) + Q_{33}^{eff}\langle P_3^2\rangle . \qquad (7)$$

Here we introduced the effective coefficients $s_{33}^{eff} = s_{33} - 2s_{13}^2/(s_{11}+s_{12})$, $W_{33}^{eff} = W_{33}^{d} - 2s_{13}W_{11}^{d}/(s_{11}+s_{12})$, $\Sigma_{33}^{eff} = \Sigma_{33}^{e} - 2s_{13}\Sigma_{11}^{e}/(s_{11}+s_{12})$, $F_{33}^{eff} = F_{33} - 2s_{13}F_{13}/(s_{11}+s_{12})$ and $Q_{33}^{eff} = Q_{33} - 2s_{13}Q_{13}/(s_{11}+s_{12})$. Voigt notations are introduced for the electrostriction Q_{ij}, gradient coefficient g_{ij}, flexoelectric F_{ij} and elastic compliance s_{ij} tensors, while full matrix notations are retained for all other tensors. The tensor

components with subscripts 12, 13 and 23 are equal for materials with cubic parent phase. Corresponding effective elastic compliance can be calculated from the formulae:

$$S_{33}^{eff} = -\frac{1}{h}\frac{du_3}{dp_{ext}}. \tag{8}$$

By definition, effective piezo-response is given by expression $R_3^{eff} = \frac{\partial u_3}{\partial V}$. Since $P_i = -\frac{\delta G}{\delta E_i}$ and $u_{ij} = -\frac{\delta G}{\delta \sigma_{ij}}$, in accordance with Maxwell relations we obtained that

$$R_3^{eff} = \frac{\partial u_3}{\partial V} = \frac{\partial P_3}{\partial p_{ext}} \equiv \frac{\partial^2 G}{\partial V \partial p_{ext}}. \tag{9}$$

Derivation of relation (9) along with approximate analytical expressions of effective piezo-response is disclosed in the **Appendixes E and C** of **Suppl. Mat.** [54]

In order to study the dependence of the film electro-conductance **Ω** on applied pressure p_{ext}, i.e. the effective piezo-conductance $\Omega_p \equiv d\Omega/dp_{ext}$, one should solve the dynamic problem and calculate a derivative of the electric current with respect to the applied voltage and study this value in dependence on p_{ext}, $\Omega_p \equiv \frac{1}{E_{ext}}\frac{\partial J}{\partial p_{ext}}$, here $E_{ext} = V/h$ (assuming linear approximation on V). The donor current is $J_d = -eZ_d \eta_d N_d^+ \left(\partial \zeta_d / \partial x_3\right)$, where η_d is the donor mobility coefficient, ζ_d is electrochemical potential for donor, $\zeta_d = -\left(\delta G/\delta N_d^+\right) \equiv E_d + W_{ij}^d \sigma_{ij} - eZ_d\varphi - k_B T \ln\left(N_d^+ / \left(N_d^0 - N_d^+\right)\right)$. The electronic current is $J_e = e\eta_e n\left(\partial \zeta_e / \partial x_3\right)$, where η_e is the electron mobility coefficient, ζ_e is electrochemical potential for electron, $\zeta_e = +\left(\delta G/\delta n\right) \equiv E_C - \Sigma_{ij}^e \sigma_{ij} + k_B T F_{1/2}^{-1}\left(n/N_C\right) - e\varphi$.

Kinetic equations for electrons and donors, $\frac{\partial n}{\partial t} - \frac{1}{e}\frac{\partial J_3^e}{\partial x_3} = 0$ and $\frac{\partial N_d^+}{\partial t} + \frac{1}{eZ_d}\frac{\partial J_d}{\partial x_3} = 0$, are supplemented by ion-blocking boundary conditions $J_d\big|_{x_3=0,h} = 0$; and fixed electron densities at the electrodes $n(0) = n_0$ and $n(h) = n_1$. For the case of ion-blocking electrodes only electronic current contributes into the conductance **Ω**. Hence the piezo-conductance can be estimated as (see **Appendix D** of **Suppl. Mat.** [54]**):**

$$\Omega_p \equiv \frac{1}{E_{ext}}\frac{dJ}{dp_{ext}} \approx e^2 \frac{\eta_e}{h}\frac{d}{dp_{ext}}\int_0^h n dx_3 \sim \frac{d\langle n \rangle}{dp_{ext}}, \tag{10}$$

Below we compare approximate analytical expressions derived in the **Suppl. Mat** [54] with self-consistent numerical modelling with and without flexoelectric coupling and pressure application.

III. Results of self-consistent calculations and discussion

Size effects of the spontaneous polarization, effective piezo-response, average elastic strain and compliance, electron concentration and piezo-conductance have been calculated in a self-consistent way for $PbZr_{0.5}Ti_{0.5}O_3$ (PZT) at room temperature (RT)**.** Parameters used are listed in the **Table I.**

Table I. Material parameters collected and estimated from the Refs [30, 62, 63]

coefficient	**$PbZr_{0.5}Ti_{0.5}O_3$**
ε_{33}^{b}	10
α^{T} **(×10^{5}C^{-2}·Jm/K)**	2.66
T_C **(K)**	666
b_{ij} **(×10^{8}C^{-4}·m^{5}J)**	b_{33}= 3.98
Q_{ij} **(C^{-2}·m^4)**	Q_{33}=Q_{11}=0.0812, Q_{13}= –0.0295
s_{ij} **(×10^{-12} Pa^{-1})**	s_{33}=s_{11}=8.2, s_{13}= -2.6'
g_{ij} **(×10^{-10}C^{-2}m^{3}J)**	g_{33}=5.0
A^{Si} **(×10^{-4}C^{-2}·J)**	A^{S1} = 1, A^{S2} = 20000
F_{ij} **(×10^{-11}C^{-1}m^3)**	F_{33}= 3, F_{13}= 0 – 3
W **(10^{-30}m^3)**	3
E_d **(eV)**	–0.1
N_d^0 **(m^{-3})**	10^{25}
Σ (eV)	0.1
Universal constants	e=1.6×10^{-19} C, ε_0=8.85×10^{-12} F/m

Corresponding dependences of the spontaneous polarization, effective piezo-response, average strain and elastic compliance, electron concentration and piezo-conductance on the film thickness h are shown in **Figures 2 - 4** Calculated curves appeared very slightly sensitive to the Vegard contribution, which coefficient W was varied in the reasonable range (0 – 10) Å^3 [64] (compare left (a,c) and right (b,d) columns in **Figures 2-4**). Weak sensitivity to the Vegard strains originated from the donor-blocking boundary conditions used in the 1D numerical modelling, which mean that the full quantity of donors is conserved between the blocking interfaces. The condition minimizes the pure Vegard contribution and does not affect the flexocoupling. Note however, that the Vegard contribution to FeMIEC response can be very important in 2D-geometry [26].

Dotted and solid curves, calculated at zero and nonzero flexoelectric coupling constants F_{ij} correspondingly, are very similar at zero external pressure, but become strongly different under external pressure application of $\pm 10^9$ Pa. At that the difference becomes noticeably stronger for compression (p_{ext}>0) than for extension (p_{ext}<0).

Without flexoelectric coupling, the main origin of the curve asymmetry occurring after the application of positive or negative pressure is that the linear renormalization of the coefficient a_{33} .

Namely, $a_{33}^{eff} = \alpha_{33}^{T}(T - T_c) + 2Q_{33}^{eff} p_{ext}$, where the last term increases or decreases a_{33}^{eff} depending on the p_{ext} sign. The coefficient a_{33}^{eff} defines the critical thickness h_{cr} as,

$$h_{cr} = -\frac{g_{33}^{eff}}{a_{33}^{eff}}\left(\frac{1}{\lambda_1 + L_C} + \frac{1}{\lambda_2 + L_C}\right), \tag{11}$$

where the renormalized gradient coefficient $g_{33}^{eff} = g_{33} + 2F_{13}^2/(s_{11} + s_{13})$, correlation and different extrapolation lengths [65, 66], $L_C = \sqrt{g_{33}^{eff}\varepsilon_0\varepsilon_{33}^{b}}$ and $\lambda_m = g_{33}^{eff} / A_{33}^{Sm}$ (**Appendix B** of **Suppl. Mat**. [54]). The approximate expression (11) is valid with high accuracy at small concentration of free carriers

Thus, the flexoelectric coupling renormalizes the gradient coefficient and consequently the extrapolation and correlation lengths [38]. Due to the linear dependence of a_{33}^{eff} on p_{ext} the critical thickness becomes dependent on p_{ext} as $h_{cr} \sim -\frac{1}{\alpha_{33}^{T}(T - T_c) + 2Q_{33}^{eff} p_{ext}}$. The dependences $h_{cr}(p_{ext})$ and $a_{33}^{eff}(p_{ext})$, which are strongly "asymmetric" function of p_{ext} lead to the asymmetry of the spontaneous polarization thickness dependences occurring after the application of positive or negative pressure (see different curves in Figures 2a and 2b).

However, the asymmetry form of the effective piezo-response and average strain is rather complex and not defined only by the asymmetry of $a_{33}^{eff}(p_{ext})$ and $h_{cr}(p_{ext})$. In accordance with Eqs.(6), (7), (B.1c) and their solution (B.2), the strain is proportional to $s_{33}^{eff} p_{ext} + Q_{33}^{eff} P_3^2$ at zero $F_{33}^{eff} = 0$, where the pressure dependence is present via the linear contribution $s_{33}^{eff} p_{ext}$, and the nonlinear one $Q_{33}^{eff} P_3^2$, because the polarization is pressure-dependent. Hence the influence of pressure sign on the strain becomes very complex and it causes the complex asymmetric dependence of the effective piezo-response on applied pressure.

Without flexoelectric coupling all physical quantities depicted in the **Figures 2 - 4** manifest noticeable peculiarities at the critical thickness $h = h_{cr}$. Since $Q_{33}^{eff} > 0$ for PZT, negative p_{ext}<0 decreases the critical thickness h_{cr}, while positive p_{ext}>0 leads to an opposite trend. Therefore $h_{cr}(p_{ext} < 0) < h_{cr}(p_{ext} = 0) < h_{cr}(p_{ext} > 0)$ (compare red, black and blue dashed curves in **Figures 2-4** corresponding to p_{ext} = –1 GPa, 0, +1 GPa and F_{ij} = 0).

The spontaneous polarization, calculated at $F_{ij} = 0$, emerges at the critical thickness h_{cr}, then increases and saturates under the film thickness increasing in a semi-quantitative agreement with the analytical formula $P_3^S = P_S^{bulk}\sqrt{1 - h_{cr}/h}$ [45] (see dashed curves in **Figures 2 a,b**). Effective piezo-response R_3^{eff} calculated at $F_{ij} = 0$ has a divergence at $h = h_{cr}$ and disappears in a paraelectric phase (see dashed curves in **Figures 2 c-d**). The behavior of R_3^{eff} is in agreement with the analytical

expression derived in the **Appendix C** of **Suppl. Mat** [54], $R_3^{piezo} = d_{33}^{PR}\sqrt{1-\frac{h_{cr}}{h}}\left(\frac{\theta(h_{cr}/h)}{|1-h_{cr}/h|}+\frac{\varepsilon_{33}^{b}}{\varepsilon_{33}^{sm}}\right)$, where the piezoresponse amplitude $d_{33}^{PR} \approx 2\varepsilon_0\varepsilon_{33}^{sm}P_S Q_{33}^{eff}$ and the function $\theta(h_{cr}/h)=2$ at $h<h_{cr}$ and $\theta(h_{cr}/h)=1$ at $h \geq h_{cr}$.

When the flexoelectric coupling is present, the boundary conditions for polarization (see **Suppl. Mat** [54], Eqs. (B.4)) contain the terms proportional to the "surface" polarizations $P_m^{BI} = F_{33}^{eff} p_{ext} / A_{33}^{Sm}$, which for chosen geometry is equivalent to a built-in electric field $E^{BI} \sim \left(P_1^{BI} - P_2^{BI}\right)/h \sim F_{33}^{eff} p_{ext}/h$. The field is inversely proportional to the thickness *h*, so its influence is significant for thin films. Since the field increases for thinner films, it smears the phase transition with decreasing *h*. The change of the applied pressure sign leads to the reversal of the surface field. In thin films, the pressure-sensitive surface field causes the situation when only one sign of polarization ($+P_S$ or $-P_S$) is stable for a given pressure sign. Note a quantitative similarity between this effect and polarization reversal and phase transition smearing due to the adsorption of surface ions under the condition of partial oxygen pressure excess [67, 68]. Negative polarization produces negative strain and negative piezo-response at positive applied pressure [see blue curves in **Figures 2a and 2b**].

The built-in field E^{BI} destroys the thickness-induced phase transition to a paraelectric phase at $h = h_{cr}$ and instead induces an electret-like state with irreversible spontaneous polarization at $h < h_{cr}$ (see solid curves in **Figures 2 a-b**). Piezo-response R_3^{eff} calculated from Eq.(9) appeared nonzero in the electret-like state at $h < h_{cr}$ and monotonically decreases with decreasing *h* (see solid curves in **Figures 2 c-d**). Finally, we observe that piezo-response calculated for positive pressure changes its sign at nonzero flexoelectric coupling [see blue curves in **Figures 2c and 2d**]. According to Eq.(7), there are two contributions in piezo-response, $\Delta\frac{\partial u_3^{piezo}}{\partial V} \sim \frac{F_{33}^{eff}}{h}(\chi_3(h)-\chi_3(0)) + Q_{33}^{eff}\langle 2P_3\chi_3\rangle$, where the linear susceptibility $\chi_3 = \partial P_3 / \partial E_3$ is introduced. The first term, that is the direct contribution of flexo-effect, does not change its sign if the sign of $P_S \sim p_{ext}$ changes, while the second term being the linearized electrostriction contribution (i.e. piezoelectric term appeared in a ferroelectric phase), changes the sign in such a situation. Flexoelectric contribution can dominate for very thin films of thickness less than the critical one, while the piezoelectric contribution becomes the main one with the film thickness increase. Consequently, when the external pressure changes its sign to positive it induces reversal of polarization in thin films, the two contributions of piezo-response add up, while in the case of zero or negative pressure they are deducted.

The spontaneous average strain $\langle u_{33} \rangle$ calculated for $F_{ij} = 0$ and $p_{ext} = 0$ emerges at the critical thickness h_{cr}, then it increases and saturates under the film thickness increasing as $\sqrt{1 - h_{cr}/h}$. Nonzero pressure shifts the strain by a constant value $-s_{33}^{eff} p_{ext}$ in accordance with Eq.(6) (compare different dashed curves in **Figure 3 a,b**). Being the derivative of the strain with respect to the applied pressure, effective compliance S_{33}^{eff}, calculated at $F_{ij} = 0$ from Eq.(8), has a sharp maximum at $h = h_{cr}$ and drops to a constant value s_{33}^{eff} in the paraelectric phase (see dashed curves in **Figure 3 c-d**).

The built-in field, produced by the joint action of flexocoupling and external pressure, destroys the thickness-induced phase transition at $h = h_{cr}$ and, rather unexpectedly, induces a noticeable increase of the absolute value of strain $|\langle u_{33} \rangle|$ for films of subcritical thickness (see solid curves in **Figure 3 a-b**). It appears that the increase is caused by the flexoelectric term $(P_3(h) - P_3(0))F_{33}^{eff}/h$ in Eq.(5) that scales as 1/*h* at small thicknesses. The term is conditioned by different build-in surface polarizations and can be estimated as $(P_2^{BI} - P_1^{BI})F_{33}^{eff}/h$. Flexoeffect leads to the very pronounced increase of the compliance S_{33}^{eff} with thickness decrease at $h < h_{cr}$ (see solid curves in **Figures 3 c-d**). In both cases ($p_{ext} < 0$ and $p_{ext} > 0$) the sharp fall in compliance with a decrease in film thickness is due to the decrease of polarization. Since the compliance is an even function of polarization, this effect does not depend on the sign of the polarization and therefore on the external pressure sign.

Without flexoelectric coupling the average electron concentration $\langle n \rangle$ starts to differ from the equilibrium bulk value $n_0 = N_C F_{1/2}((E_F - E_C)/k_B T)$ for film thickness $h > h_{cr}$, because the spontaneous polarization appears above the critical thickness and start to affect on $\langle n \rangle$ via the deformation potential and depolarization field that is produced by the $div(\vec{P}^S)$. For $p_{ext} = 1$ GPa concentration $\langle n \rangle$ grows by order of magnitude compared to base level n_0 at $h > h_{cr}$ and then saturates under the film thickness increasing. For $p_{ext} = 0$ the concentration $\langle n \rangle$ becomes about one order of magnitude smaller than n_0 at $h > h_{cr}$, while it gets two orders of magnitude smaller than n_0 at $h > h_{cr}$ for $p_{ext} = -1$GPa, then it reaches a very flat minimum and subsequently slightly increases under the film thickness increasing (see dashed curves in **Figures 4 a,b**). Effective piezo-conductance Ω_p calculated from Eq.(8) at $F_{ij} = 0$ has a divergence at $h = h_{cr}$ and abruptly disappears in a paraelectric phase at $h < h_{cr}$ (see dashed curves in **Figures 4 c-d**). The pressure induced changes of electron concentration are related with the linear renormalization of the coefficient a_{33}^{eff} by the pressure, $a_{33}^{eff} = \alpha_{33}^{T}(T - T_c) + 2Q_{33}^{eff} p_{ext}$, since the amplitude

of the spontaneous polarization $\vec{P}^S$ depends on a_{33}^{eff} in accordance with LGD-type Euler-Lagrange equation (B.3) listed in the **Appendix B** of **Suppl. Mat** [54]**.**

When the flexoelectric coupling is present it causes the built-in field $E^{BI} \sim F_{33}^{eff} p_{ext}/h$, that in turn induces noticeable deviation of $\langle n \rangle$ from the value n_0 for all film thicknesses h, including the range of small thickness $h \le h_{cr}$. Furthermore, two peculiarities are present on the thickness dependence of $\langle n \rangle$, namely flat extrema at $h \approx h_{cr}$ followed by inflexion point and then by a sharp drop to n_0 value under the film thickness decrease (see solid curves in **Figures 4 a-b**). Therefore effective piezo-conductance Ω_p, being the pressure derivative of $\langle n \rangle$ in accordance with Eq.(8), is nonzero for all film thicknesses h and reveals non-trivial thickness dependence at $p_{ext} \neq 0$ (see solid curves in **Figures 4 c-d**). For $p_{ext} = 1$GPa the piezo-conductance thickness dependence, $\Omega_p(h)$, has two maxima. The first is smeared and located at $h \approx h_{cr}$, whereas the other one is flat and located at $h < h_{cr}$. They are separated by a sharp drop (by an order of magnitude), which position corresponds to the inflection point of $\langle n \rangle$. For $p_{ext} = 0$ the dependence $\Omega_p(h)$ has one sharp maximum at $h = h_{cr}$ followed by an inflexion point; after that the rapid decrease of the dependence $\Omega_p(h)$ occurs with h decrease. For $p_{ext} = -1$GPa $\Omega_p(h)$ reaches a plateau at $h < h_{cr}$ that continues up to the ultra-small thickness. The physical origin of the non-trivial peculiarities of the effective piezo-conductance thickness dependence is the interplay of the h-dependent built-in field and polarization contributions to the electronic state.

Note that the biggest differences $\langle n(p_{ext} > 0) - n(p_{ext} < 0) \rangle$ and $\langle \Omega_p(p_{ext} > 0) - \Omega_p(p_{ext} < 0) \rangle$ (more than 3 orders of magnitude for the pressure difference 2 GPa) correspond to the film thickness $h \sim h_{cr}$ (see vertical green double arrows in **Figures 4a-b**). The changes of $\langle n \rangle$ by orders of magnitude under application of positive and negative pressures can indicate the appearance of high-conductivity (HC) and low-conductivity (LC) states in a thin film with thickness a bit higher than h_{cr}, in which swing can be ruled by flexoelectric coupling. Using the analogy with mechanical control of electro-resistive switching in MIECs (piezo-chemical effect) [18], the predicted effect makes it possible to control the non-volatile electro-resistive switching in FeMICs by changing the film thickness, external pressure and flexoelectric coupling.

The impact of the Vegard mechanism on the size effects is weak in comparison with the flexoelectric coupling, but the thickness dependence of the piezo-conductance allows one to see the difference between $W = 0$ and $W = 3$ Å^3 by comparison of **Figure 4 c** and **4d**.

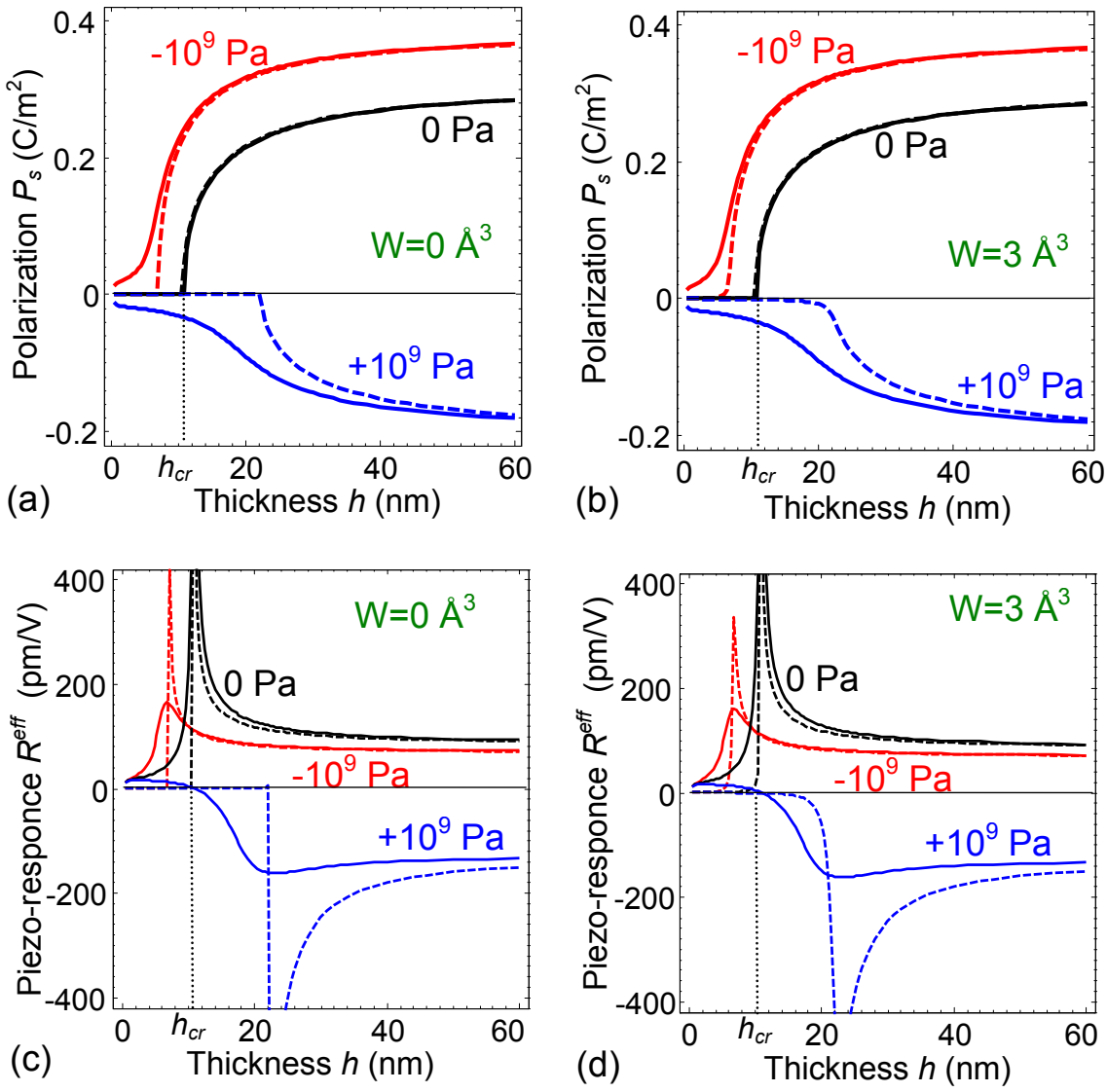

Figure 2. Thickness dependence of the average spontaneous polarization P_3^S **(a, b)** and effective piezo-response R_3^{eff} **(c, d)** of ferroelectric $PbZr_{0.5}Ti_{0.5}O_3$ calculated at RT for different values of external pressure $p_{ext} = -10^9$ Pa, 0, $+10^9$ Pa (shown near the curves) and flexoelectric coefficients F_{13}=F_{33}=0 (dashed curves); $F_{13}=1\times10^{-11}$ m^3/C, $F_{33}=3\times10^{-11}$ m^3/C (solid curves). Vegard coefficient is W=0 Å^3 **(a, c)** and W=3 Å^3 **(b, d)**. Other parameters are listed in **Table I**.

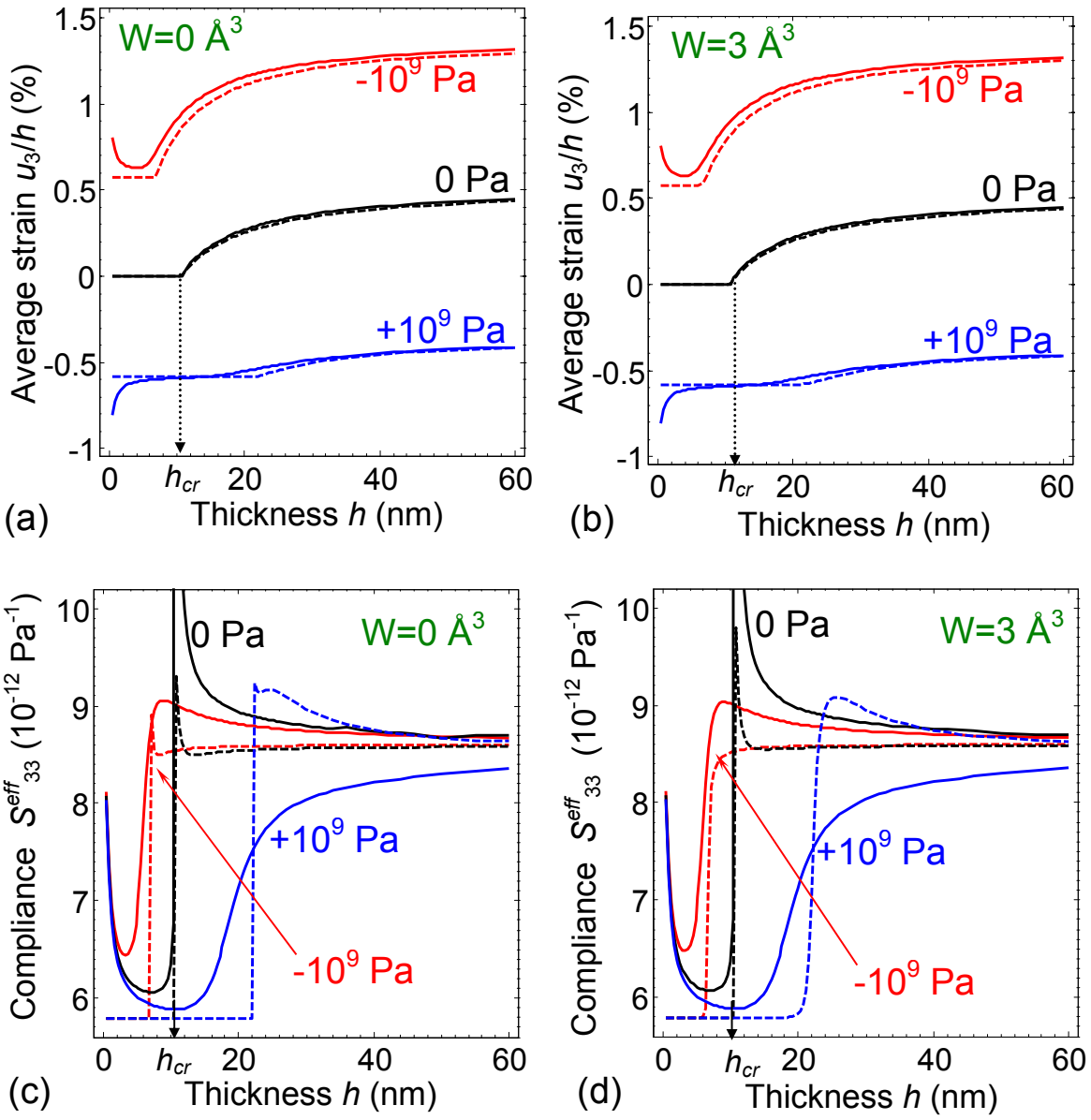

Figure 3. Thickness dependence of average strain $\langle u_{33} \rangle$ **(a, b)** and effective elastic compliance S_{33}^{eff} **(c, d)** of ferroelectric $PbZr_{0.5}Ti_{0.5}O_3$ calculated at RT for different values of external pressure $p_{ext} = -10^9$ Pa, 0, $+10^9$ Pa (shown near the curves) and flexoelectric coefficients $F_{13}=F_{33}=0$ (dashed curves); $F_{13}=1\times10^{-11}$ m^3/C, $F_{33}=3\times10^{-11}$ m^3/C (solid curves). Vegard coefficient is W=0 Å^3 (a, c) and W=3 Å^3 (b, d). Other parameters are listed in **Table I**.

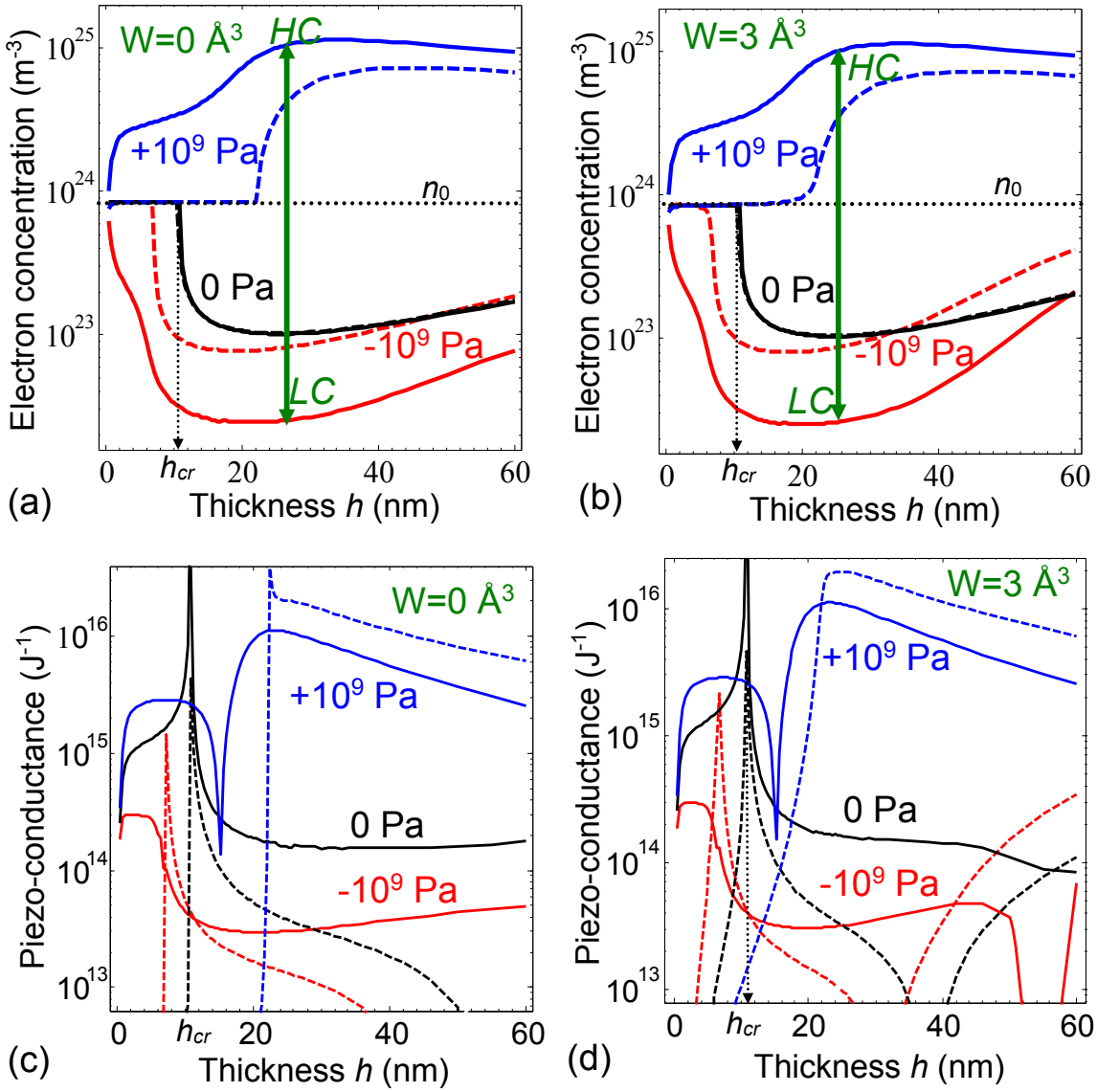

Figure 4. Thickness dependence of the average electron concentration $\langle n \rangle$ **(a, b)** and effective piezo-conductance Ω_p **(c, d)** of ferroelectric $PbZr_{0.5}Ti_{0.5}O_3$ calculated at RT for different values of external pressure $p_{ext} = -10^9$ Pa, 0, $+10^9$ Pa (shown near the curves) and flexoelectric coefficients $F_{13}=F_{33}=0$ (dashed curves); $F_{13}=1\times10^{-11}$ m^3/C, $F_{33}=3\times10^{-11}$ m^3/C (solid curves). Green arrows indicate the difference between high-conductivity (HC) and low-conductivity (LC) states. Vegard coefficient is W=0 Å^3 (a, c) and W=3 Å^3 (b, d). Other parameters are listed in **Table I**.

Our theoretical results and predictions can be verified by direct comparison to experimental data obtained in thin ferroelectric-semiconductor films by advanced PFM and C-AFM methods. In particular the dependences of the effective piezo-response and piezo-conductance measured simultaneously (i.e. *in situ*) for different film thicknesses at different applied pressures are required. In principle, the current state-of-the-art allows such studies, and we hope that the developed theoretical framework will stimulate

further studies. Furthermore, derived expressions for the strain field, effective elastic compliance, piezo-response and piezo-conductance (see e.g. Eqs.(7)-(10)), which include the dependence on the film thickness, built-in field, external pressure and flexoelectric coefficients, can be used for optimization of the thin ferroelectric film parameters to reach better performances and so they can quantitatively rationalize future experimental observations.

IV. Conclusion

Flexocoupling impact on the size effects of the spontaneous polarization, effective piezo-response, elastic strain and compliance, carrier concentration and piezo-conductance have been calculated in thin films of ferroelectric mixed-type semiconductors within LGD-approach combined with classical electrodynamics and semiconductor properties description. Analysis of the self-consistent calculation results revealed that the thickness dependences of aforementioned physical quantities, calculated at zero and nonzero flexoelectric coupling, are very similar without applied pressure, but become strongly different under the application of external pressure p_{ext}.

Without flexoelectric coupling the studied physical quantities manifest pronounced peculiarities (disappearance, divergences or sharp maxima, breaks) if the film thickness h approaches the critical thickness h_{cr} of the ferroelectricity existence. We derived analytically how the value of h_{cr} depends on the flexocoupling constants, applied pressure p_{ext}, surface energy coefficients and material parameters. Negative pressure $p_{ext}<0$ decreases the critical thickness h_{cr} while a positive one $p_{ext}>0$ leads to an opposite trend.

The combined effect of flexoelectric coupling and external pressure induces the polarizations at the film surfaces. The surface polarizations cause the built-in field that destroys the thickness-induced phase transition to the paraelectric phase at $h = h_{cr}$ and induces the electret-like state with irreversible spontaneous polarization at $h < h_{cr}$. The built-in field leads to the noticeable increase of the average strain and elastic compliance under the film thickness decrease below h_{cr} that scales as $1/h$ at small thicknesses h. The increase is conditioned by different build-in surface polarizations at small enough extrapolation lengths, since corresponding built-in field $E^{BI} \sim F_{33}^{eff} p_{ext}/h$ scales as $1/h$ at small thicknesses h (F_{33}^{eff} is the effective flexocoupling constant).

The built-in field induces non-monotonic thickness dependence of free electron density $\langle n \rangle$ for all film thicknesses h including the range of small thickness $h \le h_{cr}$. Corresponding effective piezo-conductance Ω_p is nonzero for all film thicknesses h and its thickness dependence is non-monotonic and non-trivial. The physical origin of the peculiarities of the electron concentration and effective piezo-conductance thickness dependences is the interplay of the h-dependent built-in field and polarization

impact on the electronic state. The impact of the Vegard mechanism on the size effects is weak as anticipated for the donor-blocking boundary conditions, but its influence on the thickness dependence of the piezo-conductance is notable.

The changes of $\langle n \rangle$ and Ω_p by 3 orders of magnitude under application of positive and negative external pressure of 1 GPa can indicate the appearance of high- and low- conductivity states in a thin film with thickness a bit higher than h_{cr}, which swing can be ruled by pressure magnitude and flexoelectric coupling. The predicted effect can pave the way for the size effect control of piezo-resistive switching in FeMIECs facilitated by flexoelectric coupling.

Obtained theoretical results can be of fundamental and applied interest for the thin ferroic films physics, semiconductor physics, modern interferometry and Scanning Probe Microscopy development. Predicted non-trivial behavior of the elastic properties and piezo-conductance are waiting for experimental verification by modern SPM and precise interferometry methods.

Acknowledgements

E.A.E. and A.N.M. acknowledge National Academy of Sciences of Ukraine (grant 07-06-15) and CNMS2016-061. S.V.K. acknowledges Office of Basic Energy Sciences, U.S. Department of Energy. I.S.V. is grateful to the German Research Foundation for support through the grant GE 1171/7-1. M.V.S. acknowledges the grant of the President of the Russian Federation for state support of young Russian scientists-PhD (No. 14.Y30.15.2883-MK) and the project part of the State tasks in the field of scientific activity No. 11.2551.2014/K. Y.K. acknowledges that apportion of this work was supported by Basic Science Research program through the National Research Foundation of Korea funded by the Ministry of Science, ICT & Future Planning (NRF-2014R1A4A1008474).

References

[1] N. Setter, D. Damjanovic, L. Eng, G. Fox, S. Gevorgian, S. Hong, A. Kingon, H. Kohlstedt, N. Y. Park, G. B. Stephenson, I. Stolitchnov, A. K. Tagantsev, D. V. Taylor, T. Yamada and S. Streiffer, "Ferroelectric thin films: Review of materials, properties, and applications." Journal of Applied Physics 100 (5) 051606 (2006).

[2] R. Waser, Nanoelectronics and Information Technology (John Wiley & Sons, Weinheim, 2012).

[3] J. F. Scott, " Applications of modern ferroelectrics. " Science 315 (5814), 954-959 (2007).

[4] M. Fiebig, " Revival of the magnetoelectric effect. " J. Phys. D-Appl. Phys. 38 (8), R123-R152 (2005).

[5] N. A. Spaldin and M. Fiebig, " The renaissance of magnetoelectric multiferroics. " Science 309 (5733), 391-392 (2005).

[6] S. V. Kalinin and N. A. Spaldin, " Functional ion defects in transition metal oxides. " Science 341 (6148), 858-859 (2013).

[7] J. Seidel, L. W. Martin, Q. He, Q. Zhan, Y. H. Chu, A. Rother, M. E. Hawkridge, P. Maksymovych, P. Yu, M. Gajek, N. Balke, S. V. Kalinin, S. Gemming, F. Wang, G. Catalan, J. F. Scott, N. A. Spaldin, J. Orenstein and R. Ramesh, "Conduction at domain walls in oxide multiferroics." Nat. Mater. 8 (3), 229-234 (2009).

[8] S. V. Kalinin, A. Borisevich and D. Fong, "Beyond condensed matter physics on the nanoscale: the role of ionic and electrochemical phenomena in the physical functionalities of oxide materials." Acs Nano 6 (12), 10423-10437 (2012).

[9] P.S. Sankara Rama Krishnan, Anna N. Morozovska, Eugene A. Eliseev, Quentin M. Ramasse, Demie Kepaptsoglou, Wen-I Liang, Ying-Hao Chu, Paul Munroe and V. Nagarajan. "Misfit strain driven cation inter-diffusion across an epitaxial multiferroic thin film interface." J. Appl. Phys. **115**, 054103 (2014).

[10] Anna N. Morozovska, Eugene A. Eliseev, P.S.Sankara Rama Krishnan, Alexander Tselev, Evgheny Strelkov, Albina Borisevich, Olexander V. Varenyk, Nicola V. Morozovsky, Paul Munroe, Sergei V. Kalinin and Valanoor Nagarajan. "Defect thermodynamics and kinetics in thin strained ferroelectric films: The interplay of possible mechanisms." Phys. Rev. B **89**, 054102 (2014).

[11] Akihito Sawa, " Resistive switching in transition metal oxides. ". MaterialsToday, **11**, 28 (2008).

[12] D. B. Strukov, G. S. Snider, D. R. Stewart, R. S. Williams, "The missing memristor found" Nature, **453**, 80 (2008).

[13] G. Catalan and James F. Scott. "Physics and applications of bismuth ferrite." Adv. Mater. **21**, 1–23 (2009).

[14] N. Balke, S. Jesse, A.N. Morozovska, E. Eliseev, D.W. Chung, Y. Kim, L. Adamczyk, R.E. Garcıa, N. Dudney and S.V. Kalinin. "Nanoscale mapping of ion diffusion in a lithium-ion battery cathode". Nature Nanotechnology 5, 749–754. (2010).

[15] Hugues-Yanis Amanieu, Huy N.M. Thai, Sergey Yu. Luchkin, Daniele Rosato, Doru C. Lupascu, Marc-Andre Keip, Jorg Schroder, Andrei L. Kholkin, Electrochemical Strain Microscopy Time Spectroscopy: model and experiment on $LiMn_2O_4$. Accepted to JAP (2016)

[16] K. Romanyuk, C. M. Costa, S. Yu. Luchkin, A. L. Kholkin, S. Lanceros-Mendez. Giant electric field-induced strain in PVDF-based battery separator membranes probed by Electrochemical Strain Microscopy. Accepted to Langmuir (2016)

[17.] S.V. Kalinin, S. Jesse, B.J. Rodriguez, J. Shin, A.P. Baddorf, H.N. Lee, A. Borisevich, S.J. Pennycook. " Spatial resolution, information limit, and contrast transfer in piezoresponse force microscopy. " Nanotechnology **17**, 3400 (2006).

[18] Yunseok Kim, Simon J. Kelly, Anna Morozovska, Ehsan Kabiri Rahani , Evgheni Strelcov, Eugene Eliseev, Stephen Jesse, Michael D. Biegalski, Nina Balke, Nicole Benedek, Dmitri Strukov, J. Aarts, Inrok Hwang, Sungtaek Oh, Jin Sik Choi, Taekjib Choi, Bae Ho Park, Vivek B. Shenoy, Peter Maksymovych, and Sergei V. Kalinin. "Mechanical Control of Electroresistive Switching." *Nano Letters*, **13**, 4068−4074 (2013)

[19] Y. H. Hsieh, E. Strelcov, J. M. Liou, C. Y. Shen, Y. C. Chen, S. V. Kalinin and Y. H. Chu, "Electrical modulation of the local conduction at oxide tubular interfaces." Acs Nano 7 (10), 8627-8633 (2013).

[20] Y. Kim, E. Strelcov, I. R. Hwang, T. Choi, B. H. Park, S. Jesse and S. V. Kalinin, "Correlative multimodal probing of ionically-mediated electromechanical phenomena in simple oxides." Sci Rep 3, 2924 (2013).

[21] E. Strelcov, S. Jesse, Y. L. Huang, Y. C. Teng, Kravchenko, II, Y. H. Chu and S. V. Kalinin, "Space-and time-resolved mapping of ionic dynamic and electroresistive phenomena in lateral devices." Acs Nano 7 (8), 6806-6815 (2013).

[22] E. Strelcov, Y. Kim, S. Jesse, Y. Cao, I. N. Ivanov, Kravchenko, II, C. H. Wang, Y. C. Teng, L. Q. Chen, Y. H. Chu and S. V. Kalinin, "Probing local ionic dynamics in functional oxides at the nanoscale." Nano Letters 13 (8), 3455-3462 (2013).

[23]. V.S. Mashkevich, and K.B. Tolpygo, *Zh.Eksp.Teor.Fiz.* **31**, 520 (1957) [*Sov.Phys. JETP*, **4**, 455 (1957)]. see also 1957, *J. exp. theor. Phys., Moscow,* 32, 520. (Translation: *Soviet Physics, JETP,* 5, 435.)

[24] Sh. M. Kogan, "Piezoelectric effect under an inhomogeneous strain and an acoustic scattering of carriers of current in crystals "Solid State Physics, Vol. **5**, 10, 2829 (1963)

[25] A.N. Morozovska, E.A. Eliseev, A.K. Tagantsev, S.L. Bravina, Long-Qing Chen, and S.V. Kalinin. "Thermodynamics of electromechanically coupled mixed ionic-electronic conductors: Deformation potential, Vegard strains, and flexoelectric effect". Phys. Rev. **B 83**, 195313 (2011).

[26] A.N. Morozovska, E.A. Eliseev, G.S. Svechnikov, and S.V. Kalinin. "Nanoscale electromechanics of paraelectric materials with mobile charges: Size effects and nonlinearity of electromechanical response of $SrTiO_3$ films". Phys. Rev. **B 84**, 045402 (2011).

[27] A.N. Morozovska, E.A. Eliseev, S.V. Kalinin. " Electromechanical probing of ionic currents in energy storage materials ". Appl. Phys. Lett. 96, 222906 (2010).

[28] A.N. Morozovska, E.A. Eliseev, N. Balke, S.V. Kalinin // Local probing of ionic diffusion by electrochemical strain microscopy: spatial resolution and signal formation mechanisms / J. Appl. Phys. 108, 053712 (2010).

[29] X. Zhang, A. M. Sastry, W. Shyy, "Intercalation-induced stress and heat generation within single lithium-ion battery cathode particles." J. Electrochem. Soc. **155**, A542 (2008).

[30] Daniel A. Freedman, D. Roundy, and T. A. Arias, "Elastic effects of vacancies in strontium titanate: Short-and long-range strain fields, elastic dipole tensors, and chemical strain." Phys. Rev. B **80**, 064108 (2009).

[31] C. Herring, E. Vogh, "Transport and deformation-potential theory for many-valley semiconductors with anisotropic scattering. " Phys.Rev. **101**, 944 (1956).

[32] J. Liu, D. D. Cannon, K. Wada, Y. Ishikawa, D.T. Danielson, S. Jongthammanurak, J. Michel, and L.C. Kimerling. "Deformation potential constants of biaxially tensile stressed Ge epitaxial films on Si (100)". Phys. Rev. B **70**, 155309 (2004).

[33] P V Yudin and A K Tagantsev. Fundamentals of flexoelectricity in solids. Nanotechnology, 24, 432001 (2013).

[34] Sergei V. Kalinin and Anna N. Morozovska. Multiferroics: focusing the light on flexoelectricity. NatureNanotechnology 10, 916–917 (2015).

[35] Alexander K. Tagantsev, L. Eric Cross, and Jan Fousek. *Domains in Ferroic Crystals and Thin Films*. (Springer New York, 2010)

[36] G. Catalan, L.J. Sinnamon and J.M. Gregg The effect of flexoelectricity on the dielectric properties of inhomogeneously strained ferroelectric thin films J. Phys.: Condens. Matter **16**, 2253 (2004).

[37] M. S.Majdoub, R. Maranganti, and P. Sharma. "Understanding the origins of the intrinsic dead layer effect in nanocapacitors." Phys. Rev. *B* 79, no. 11: 115412 (2009).

[38] E.A. Eliseev, A.N. Morozovska, M.D. Glinchuk, and R. Blinc. Spontaneous flexoelectric/flexomagnetic effect in nanoferroics / Phys. Rev. B. **79**, № 16, 165433-1-10, (2009).

[39] Andrei Kholkin, Igor Bdikin, Tetyana Ostapchuk, and Jan Petzelt. "Room temperature surface piezoelectricity in SrTiO3 ceramics via piezoresponse force microscopy." *Applied Physics Letters* **93**, 222905 (2008)

[40] R. Tararam, I. K. Bdikin, N. Panwar, José Arana Varela, P. R. Bueno, and A. L. Kholkin. "Nanoscale electromechanical properties of CaCu3Ti4O12 ceramics." *Journal of Applied Physics* **110**(5), 052019 (2011).

[41] S. V. Kalinin, S. Jesse, W. L. Liu and A. A. Balandin, "Evidence for possible flexoelectricity in tobacco mosaic viruses used as nanotemplates." Appl. Phys. Lett. 88 (15) 153902 (2**006).**

[42] S.V. Kalinin, B.J. Rodriguez, J. Shin, S. Jesse, V. Grichko, T. Thundat, A.P. Baddorf, and A. Gruverman "Bioelectromechanical imaging by scanning probe microscopy: Galvani's experiment at the nanoscale". Ultramicroscopy. **106**, (4-5), 334-340 (2006)

[43] A. Biancoli, C. M. Fancher, J. L. Jones, and D. Damjanovic. "Breaking of macroscopic centric symmetry in paraelectric phases of ferroelectric materials and implications for flexoelectricity." *Nature materials* **14**, no. 2 (2015): 224-229.

[44] Tilley D.R. Finite-size effects on phase transitions in ferroelectrics. Ferroelectic Thin Films / ed. C. Paz de Araujo, J.F.Scott and G.W. Teylor.-Amsterdam: Gordon and Breach, 1996.-P.11-4

[45] M.D.Glinchuk, E.A. Eliseev, V.A. Stephanovich, R. Fahri. Ferroelectric thin films properties - Depolarization field and renormalization of a "bulk" free energy coefficients. J. Appl. Phys Vol. 93, № 2, 1150–1159 (2003).

[46] M.D. Glinchuk, A.N. Morozovska. The internal electric field originating from the mismatch effect and its influence on ferroelectric thin film properties / J. Phys.: Condens. Matter Vol. 16, № 21, 3517–3531 (2004).

[47] M.D. Glinchuk, A.N. Morozovska, E.A. Eliseev. Ferroelectric thin films phase diagrams with self-polarized phase and electret state. J. Appl. Phys. 99, № 11, 114102-1-12. (2006).

[48] A.N. Morozovska, E.A. Eliseev, S.V. Svechnikov, A.D. Krutov, V.Y. Shur, A.Y. Borisevich, P. Maksymovych, S.V. Kalinin. Finite size and intrinsic field effect on the polar-active properties of ferroelectric semiconductor heterostructures. Phys. Rev. B. 81, 205308 (2010).

[49]D. J. Franzbach, Y. J. Gu, L. Q. Chen, and K. G. Webber. Electric field-induced tetragonal to orthorhombic phase transitions in [110]c-oriented BaTiO3 single crystals Applied Physics Letters **101**, 232904 (2012)

[50] Daniel J. Franzbach, Bai-Xiang Xu, Ralf Mueller, and Kyle G. Webber. The effects of polarization dynamics and domain switching energies on field induced phase transformations of perovskite ferroelectrics. Applied Physics Letters 99, 162903 (2011)

[51] Maxim Y. Gureev, Alexander K. Tagantsev, and Nava Setter. "Head-to-head and tail-to-tail 180 domain walls in an isolated ferroelectric." *Physical Review B* 83, 184104 (2011).

[52] Note that we did not include the higher elastic gradient term, $\frac{1}{2} v_{ijklmn}\left(\partial \sigma_{ij}/\partial x_m\right)\left(\partial \sigma_{kl}/\partial x_n\right)$, in the functional (1a), because its value and properties are still under debate. Therefore we are subjected to use only one half ($F_{ijkl}P_k\left(\partial \sigma_{ij}/\partial x_l\right)$) of the full Lifshitz invariant $F_{ijkl}\left(P_k\left(\partial \sigma_{ij}/\partial x_l\right)-\sigma_{ij}\left(\partial P_k/\partial x_l\right)\right)/2$. The higher elastic gradient term is required for the stability of the functional with full Lifshitz invariant included. The usage of either the term $F_{ijkl}P_k\left(\partial \sigma_{ij}/\partial x_l\right)$ or the term $F_{ijkl}\left(P_k\left(\partial \sigma_{ij}/\partial x_l\right)-\sigma_{ij}\left(\partial P_k/\partial x_l\right)\right)/2$ does not affect on the equations of state, but influences on the elastic boundary conditions.

[53] Y. Gil, O. M. Umurhan, and I. Riess. " Properties of a solid state device with mobile dopants: Analytic analysis for the thin film device". J. Appl. Phys. **104**, 084504 (2008)

[54] See Supplemental Material at [URL will be inserted by publisher] for calculation details

[55] S. M. Sze, *Physics of Semiconductor Devices*, 2nd ed. (Wiley-Interscience, New York, 1981).

[56] Anna N. Morozovska, Eugene A. Eliseev, Olexandr V. Varenyk, Yunseok Kim, Evgheni Strelcov, Alexander Tselev, Nicholas V. Morozovsky, and Sergei V. Kalinin. Space charge dynamics in solid electrolytes with steric effect and Vegard stresses: resistive switching and ferroelectric-like hysteresis of electromechanical response**.** Journal of Applied Physics **116**, 066808 (2014)

[57] Chun-Gang Duan, Renat F. Sabirianov, Wai-Ning Mei, Sitaram S. Jaswal, and Evgeny Y. Tsymbal. "Interface effect on ferroelectricity at the nanoscale." Nano Letters **6**, 483 (2006). Chun-Gang Duan, S. S. Jaswal, and E.Y. Tsymbal. "Predicted magnetoelectric effect in Fe/BaTiO 3 multilayers: ferroelectric control of magnetism." Phys. Rev. Lett. **97**, 047201 (2006)

[58] Note, that the total polarization component $P_k^t(\mathbf{r})$ includes both ferroelectric contribution $P_k(\mathbf{r})$, originated from a soft mode, and non-ferroelectric one, $P_k^b(\mathbf{r})$. For both ferroelectrics and highly-polarized paraelectrics the non-ferroelectric contribution is typically much smaller than the ferroelectric one, $\left|P_k(\mathbf{r})\right| >> \left|P_k^b(\mathbf{r})\right|$. So that we can regard that $P_k^t(\mathbf{r}) \approx P_k(\mathbf{r})$ and hereinafter omit the subscript "*t*" in the term $Q_{ijkl}P_k P_l$ in Eq.(1a).

[59]G.A. Smolenskii, V.A. Bokov, V.A. Isupov, N.N Krainik, R.E. Pasynkov, A.I. Sokolov, *Ferroelectrics and Related Materials* (Gordon and Breach, New York, 1984). P. 421

[60] Sang Mo Yang, A .N. Morozovska, Rajeev Kumar, E. A. Eliseev, Ye Cao, L. Mazet, N. Balke, S. Jesse, Rama Vasudevan, C. Dubourdieu, S. V. Kalinin. Mixed electrochemical-ferroelectric states in nanoscale ferroelectrics (unpublished)

[61]. A. I. Lurie, *Spatial problems of the elasticity theory*, (Gos. Izd. Teor. Tekh. Lit., Moscow, 1955) in rus.

[62] M. J. Haun, Z.Q. Zhuang, E. Furman, S.J. Jang and L.E. Cross. "Thermodynamic theory of the lead zirconate-titanate solid solution system, part III: Curie constant and sixth-order polarization interaction dielectric stiffness coefficients."Ferroelectrics, Vol. 99, pp. 45-54 (1989).

[63] N.A. Pertsev, V.G. Kukhar, H. Kohlstedt, and R. Waser, "Phase diagrams and physical properties of single-domain epitaxial Pb (Zr 1− x Ti x) O_3 thin films." Phys. Rev. B **67**, 054107 (2003).

[64] Zhang et al [17] considered intercalation of Li and used the constant **Ω** named "the partial molar volume of lithium", determining the strain inserted by the excess concentration of lithium. They used value of **Ω** that we could recalculate to the value of $W = 1.9$ Å^3 (see Eqs. [8], [9] in ref [17]). Freedman et al [18] used a shell potential model to calculate chemical strains or elastic dipole moments for various defects in $SrTiO_3$. They obtained elastic dipole –tensor values in the range $W = (2 – 24)$Å^3 depending on the type of the defect. Hence we concluded that the W within (0-10) Å^3 can be a reasonable range.

[65] R. Kretschmer and K.Binder. " Surface effects on phase transitions in ferroelectrics and dipolar magnets. " Phys. Rev. B **20**, 1065 (1979).

[66] Chun-Lin Jia, Valanoor Nagarajan, Jia-Qing He, Lothar Houben, Tong Zhao, Ramamoorthy Ramesh, Knut Urban & Rainer Waser. " Unit-cell scale mapping of ferroelectricity and tetragonality in epitaxial ultrathin ferroelectric films." Nature Materials, **6**. 64 (2007).

[67] M. J.Highland, T. T. Fister, D. D. Fong, P. H. Fuoss, Carol Thompson, J. A. Eastman, S. K. Streiffer, and G. B. Stephenson. "Equilibrium polarization of ultrathin $PbTiO_3$ with surface compensation controlled by oxygen partial pressure." Physical Review Letters,**107**, no. 18, 187602 (2011).

[68] Stephenson, G.B. and Highland, M.J., 2011. Equilibrium and stability of polarization in ultrathin ferroelectric films with ionic surface compensation. Physical Review **B**, **84** (6), p.064107 (2011)